

## SUPPLEMENTARY

### S1. Model evaluation

We calculated net torques about individual leg joints using a rigid link model (figure 1c of the main manuscript). The use of rigid links was justified, because leg segments did not bend on a measurable scale during walking. The model neglects inertial and gravitational effects due to small segment masses and simplifies the orientation of the thorax-coxa (ThC) joint axis, the position of the coxa-trochanter (CTr) joint, and the foot's centre of pressure. We evaluated the effects of all assumptions on torque calculations by re-running our analysis for the entire data set including inertia and gravity (*a*) and using alternative leg model configurations (*b-d*). This evaluation confirmed that the simplifications made did not change the conclusions reached in the main manuscript.

#### (a) *Inertial and gravitational effects*

Our analysis considered external joint torques only and did not include torques produced by segment inertia and gravity. In larger vertebrates, this simplification can introduce substantial errors in torque magnitudes, particularly at proximal joints [1]. In smaller animals, on the other hand, these errors are typically negligible due to relatively small segment masses [2].

To confirm that inertial and gravitational effects were also negligible in our experiments, we calculated joint torques using the traditional recursive Newton-Euler algorithm. Calculations were performed in Matlab, using the *Spatial\_v2* library (R. Featherstone, see also [3]). The ThC joint was considered to be connected to a fixed base. The leg segments were modelled as homogeneous solid cylinders with the centre of mass being located at the geometrical centre of each cylinder. Corresponding inertia matrices were calculated from typical segment masses and segment dimensions of a stick insect leg (table S1). Markers on the femur and tibia (figure S1, grey spheres in leg schematic) were modelled as homogeneous solid spheres (ta-

Table S1. Morphometric data of a stick insect hind leg and motion capture marker used for the exemplary inverse dynamics calculations (figure S1).

	mass (g)	radius (m)	length (m)
coxa-trochantero-femur	$11 \cdot 10^{-3}$	$6.0 \cdot 10^{-4}$	$14.4 \cdot 10^{-3}$
tibia	$4 \cdot 10^{-3}$	$2.5 \cdot 10^{-4}$	$13.9 \cdot 10^{-3}$
marker	$4 \cdot 10^{-3}$	$7.5 \cdot 10^{-4}$	

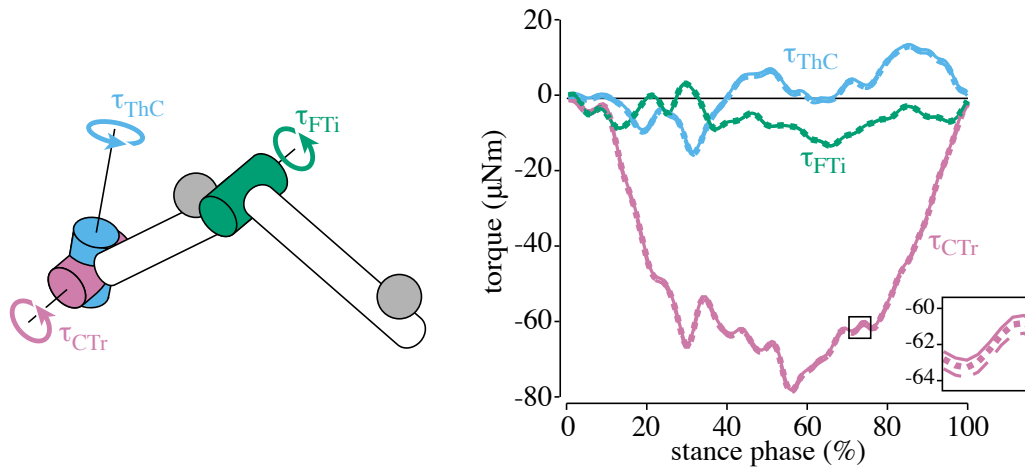


Figure S1. Effects of inertia and gravity on torque calculations about the thorax-coxa (ThC, blue), coxa-trochanter (CTr, purple), and femur-tibia (FTi, green) joint were negligible. Time courses show data of an exemplary hind leg step, neglecting all inertial and gravitational effects (solid lines, as in the main manuscript), including inertial and gravitational effects of the leg segments (dotted lines), and including inertial and gravitational effects of both the leg segments and the motion capture markers (dashed lines).

ble S1). Their positions on the leg segments were measured from high-resolution photographs prior to experimentation. The compound moment of inertia (leg segment plus marker) was determined using the parallel axis theorem. The compound centre of mass was determined from the weighted mean of the segment and marker mass.

The example calculations for a hind leg step clearly demonstrate that including inertial and gravitational effects of the leg segments and motion capture markers has no significant effect on the timing and magnitude of joint torques (figure S1). These results confirm that torques produced by segment inertia and gravity during the stance phase are small in relation to those exerted by the ground reaction force, and can indeed be neglected in our experiments.

### (b) Orientation of the thorax-coxa joint axis

The second simplification concerned the most proximal leg joint, the ThC or subcoxal joint. As in many other insect species, it is more complex than the CTr and FTi joints, which act as hinges in *C. morosus*. The dorsal side of the coxa forms a ball-and-socket-like articulation with a rounded prominence of the thorax (pleural condyle). The ventral side is attached to the thorax by the elastically articulated trochantine [4]. As a consequence, the position of the ThC joint axis is not necessarily fixed, and the joint could in principle provide a wider range of leg movements, including to some extent also levation/depression of the leg. During the stance phase of walking, however, most of the leg movement around this joint is described by the retraction and supination angles, which define the leg plane [5,6]. Both angles vary almost in

direct proportion during the stance phase, indicating that the ThC joint can be modelled as a single axis that is slanted to the side of the body within the leg plane. To estimate the angle by which the ThC joint axis ( $a_{ThC}$ ) is slanted outward, we reconstructed its orientation by intersecting leg planes at successive points in time. That is, we approximated the time course of  $a_{ThC}$  by taking the cross product of the leg plane's normal vectors ( $n$ ) at successive time points ( $t$ ) during the stance phase according to

$$a_{ThC}(t + 1) \approx n(t) \times n(t - 1) \quad (\text{S.1})$$

We used angle  $\theta$  to describe the resulting orientation of  $a_{ThC}$  relative to the vertical thorax axis ( $a_{Th}$ ) (figure S2). Figure S2a shows representative time courses of  $\theta$  for a hind, middle, and front leg step. During the portion of the stance phase in which the leg was continuously retracted (white area in figure S2a), the time courses of  $\theta$  were variable, but oscillated around  $30^\circ$ . Note that calculation artefacts occurred when the leg moved slowly—mainly directly after touchdown or before liftoff (grey areas in figure S2a). The corresponding  $\theta$ -values were not considered for evaluation.

Given that  $\theta$  varied relatively little for much of the stance phase, we simplified the kinematic calculations in our analysis and approximated the rotational axis of the ThC joint by rotating  $a_{Th}$  in the leg plane by  $\theta = 30^\circ$  in each step. To compare the resulting orientation of the joint axis with previously reported estimates [4,5], we projected the joint axis into a spherical body-fixed coordinate system. In this coordinate system, the azimuth angle  $\phi$  describes the projection of the joint axis on the horizontal body plane. This plane is spanned by the fore-aft (x) and medio-lateral (y) body axis, with  $\phi = 0^\circ$  pointing toward the head and  $\phi = 90^\circ$  pointing toward the right body side. The elevation angle  $\psi$  gives the orientation of the joint axis relative to the vertical (z) body axis, with  $\psi = 0^\circ$  indicating a vertical joint axis. For the steps shown in figure S2a, rotating  $a_{Th}$  in the leg plane by  $\theta = 30^\circ$  resulted in little movement of the joint axis (solid lines in figure S2b). The range of axis movement described by angles  $\theta$  and  $\psi$  corresponded well to earlier reported estimates for freely walking stick insects [4,5].

To estimate the effect of our choice of  $\theta$  on torque calculations at the ThC joint, we reran our analysis setting  $\theta = 0^\circ$ . For the latter, the ThC axis moved considerably (dotted lines in figure S2b). Nevertheless, the shape of the joint torque time courses remained essentially unchanged and effects on torque magnitudes were small. Effects were small both at the level of single steps (figure S2c) and grand means (figure S2d), giving us good assurance that our

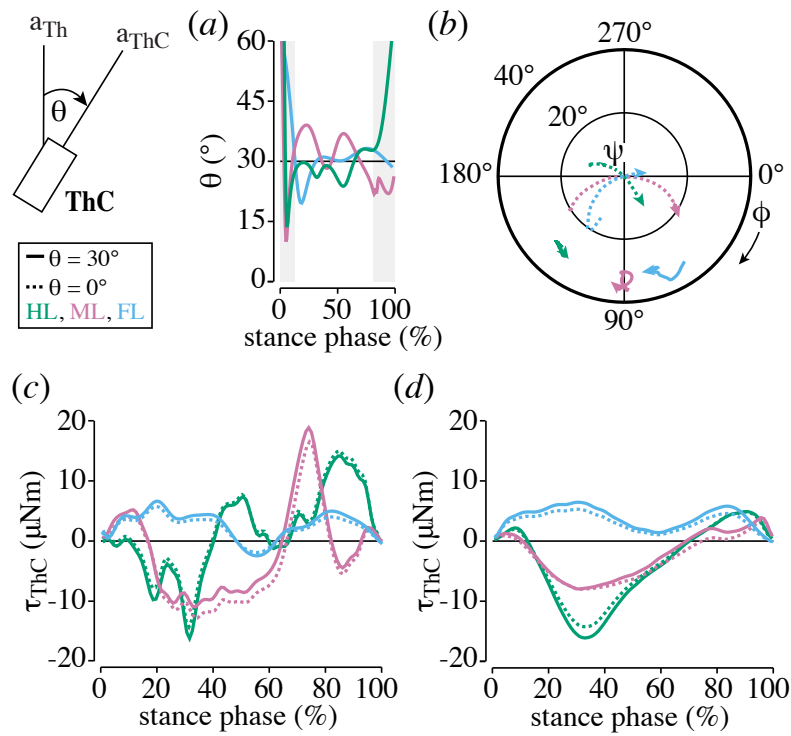


Figure S2. Estimated effects of the simplified orientation of the thorax-coxa (ThC) joint on torque time courses were small. (a) Reconstructing the angle  $\theta$ , by which the ThC joint axis is slanted within the leg plane, revealed oscillations around  $30^\circ$  in individual steps. (b) Setting  $\theta = 30^\circ$  (solid lines) in our analysis resulted in little movement of the ThC joint axis in the body-fixed coordinate system compared with  $\theta = 0^\circ$  (dotted lines). In this spherical coordinate system,  $\phi = 0^\circ$  points toward the head and  $\psi = 0^\circ$  is vertical. Lines indicate the end point of the unit vector describing the orientation of the ThC joint axis. Using  $\theta = 30^\circ$  or  $\theta = 0^\circ$  had only minor effects on joint torque calculations for both single steps (c) and grand means (d). For comparison, (a)–(c) show the same three hind leg (HL, green), middle leg (ML, purple), and front leg (FL, blue) steps.

choice of  $\theta$  did not influence the conclusions drawn from torques at the ThC joint.

As mentioned above, our leg model neglects a possible second DoF at the ThC joint that could produce torques in the direction of leg depression, similar to the CTr joint. While this assumption is common in the stick insect literature (e.g., [7,8]), the actual contribution of the ThC joint to leg depression remains unknown. If another DoF was introduced in our model, the ThC joint could assist the CTr joint in producing depression torques and thereby play a role in body support and depression-driven propulsion as well. The assumption of a single DoF for the ThC joint should therefore be re-examined in future studies. This, however, will not affect the main conclusion that propulsion is controlled by leg depression rather than leg retraction.

### ***(c) Position of the coxa-trochanter joint***

The third simplification concerned the CTr joint. It acts as a hinge connecting the coxa with the trochantero-femur segment (trochanter and femur are fused in stick insects). Rotation about the CTr joint levates or depresses the leg. In the main manuscript, we show that torques about this joint are essential to control body weight support and propulsion. Determining its exact position relative to the thorax is difficult in freely walking animals. The short length of the coxa ( $\sim 1.5$  mm) did not permit the use of a body marker (1.5 mm in diameter), as joint movements needed to be unrestrained. In principle, the joint position can be inferred from triangulation based on known segment lengths of coxa and femur along with the body marker position on the femur. However, this calculation was highly sensitive to small inaccuracies in initial length measurements, and did not result in sufficiently accurate joint positions in all steps. We therefore assumed that the CTr joint was connected directly to the thorax. This has two implications for torque calculations. First, neglecting the coxa as a moving segment effectively lumped the levation/depression of the coxa and the levation/depression of the trochantero-femur into a single joint angle estimate. While recent motion analysis of the trochantero-femur indeed suggests that most leg levation/depression is caused by rotation about the CTr joint [6], the ThC joint could assist the CTr joint in leg depression if it was modelled with an additional DoF (see above). This possibility should be re-examined in future studies. Second, re-locating the CTr joint shortened the lever arm (distance from joint to ground reaction force at the foot) by approximately the length of the coxa.

To estimate the effect of the change in lever arm on torque calculations, we re-ran our analysis with a “rigid coxa”, i.e., setting the CTr joint in constant distance to the ThC joint (figure S3). We set the distance to  $l_{cox} = 1.5$  mm, which corresponds to an average coxa length. The rotation angle of the coxa segment relative to the lateral body axis was set to  $\theta_{cox} = 45^\circ$ . As expected, the slightly shortened lever arm resulted in slightly smaller torque magnitudes, but effects on grand means were minor in all legs (figure S3). Most importantly, the shape of the time courses remained unchanged. As we consider the temporal profile to be more relevant for interpretation than exact magnitudes, the simplified position of the CTr joint was sufficiently accurate for our purposes.

### ***(d) Tibia-tarsus joint as centre of pressure***

The last simplification concerned the centre of pressure (CoP). In our leg model, we used the tibia-tarsus (TiTa) joint as an estimate. The tarsus was not tracked directly because attach-

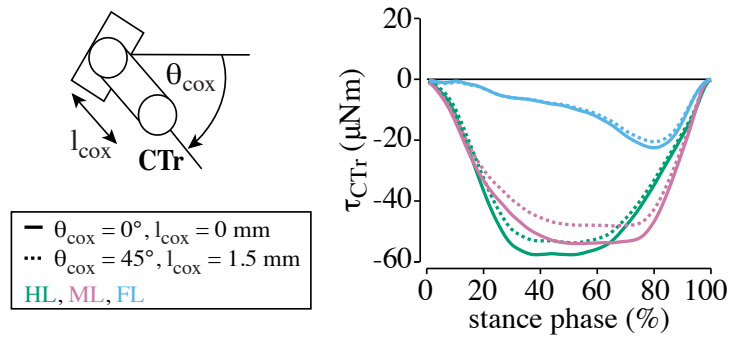


Figure S3. Estimated effects of the simplified position of the coxa-trochanter (CTr) joint on torque time courses were small. Re-running our analysis assuming a constant distance between the body and the CTr joint ( $l_{cox} = 1.5$  mm,  $\theta_{cox} = 45^\circ$ ) decreased the magnitudes of average CTr torques only moderately (dotted lines).

ing a motion capture marker to the highly flexible and multi-segmented structure would have restrained its movement. Based on our digital videos and previous reports on standing stick insects [9], the actual point of force introduction was likely the proximal part of the second tarsal segment. Changing the CoP accordingly would increase the lever arms for all joints and, in turn, affect the magnitudes of all joint torques.

To estimate the effect, we re-ran our analysis assuming that the CoP lies within the leg plane in constant distance to the TiTa joint (figure S4). We set the distance to  $l_{cop} = 2$  mm, which corresponds to the average length of a first tarsal segment. Further, we assumed a constant angle of attack relative to the ground of  $\theta_{cop} = 45^\circ$ , which corresponds to an estimated average angle based on our digital videos. The effect on torques about the ThC and CTr joints were minor (figure S4a,b). Effects were more pronounced at the FTi joint, particularly in middle legs (figure S4c), but the conclusions reached in the main manuscript remain unaffected. There, we demonstrate that torques about the middle leg's FTi joint were most variable and highly sensitive to the current leg posture. This result holds even when assuming a different CoP (figure S4d). To confirm that variability at the middle leg's FTi joint did not result from assuming a fixed CoP position, we re-ran our analysis assuming randomly varying CoP positions. We varied the CoP either from step to step or from frame to frame within steps, using random combinations of  $l_{cop} = \{1,2,3,4\}$  mm and  $\theta_{cop} = \{30,45,60\}^\circ$ . The effects on joint torque time courses and the correlation at the middle leg's FTi joint were similar to assuming a systematic variation of the CoP (figure S4).

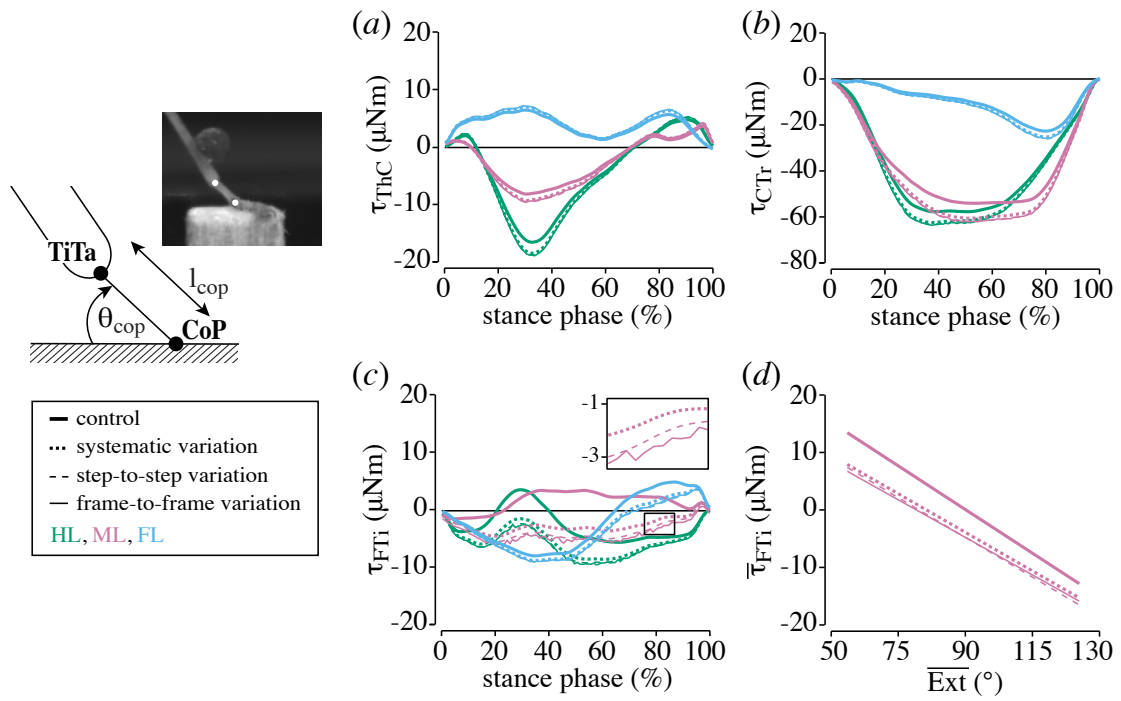


Figure S4. Estimated effects of the simplified position of the centre of pressure (CoP) on torque calculations at the thorax-coxa (ThC), coxa-trochanter (CTr), and femur-tibia (FTi) joint. Re-running our analysis assuming a constant distance between the tibia-tarsus (TiTa) joint and the actual CoP in all steps (dotted lines;  $l_{cop} = 2$  mm,  $\theta_{cop} = 45^{\circ}$ ) had only minor effects on average torques at the ThC and CTr joints (a,b). The effect was strongest at the middle leg's FTi joint (c), but the correlation between torque magnitude and tibia orientation remained significant (d). Varying the CoP randomly ( $l_{cop} = \{1,2,3,4\}$  mm,  $\theta_{cop} = \{30,45,60\}^{\circ}$ ) from step to step (dashed lines) or from frame to frame within steps (thin solid lines) had a similar effect.

## S2. Supplementary results and discussion

### (a) Correlations between joint torques and leg forces

Table S2. Correlations between time courses of joint torques and leg forces (grand means).<sup>a</sup>

	hind leg		middle leg		front leg	
	<i>r</i> -value	<i>p</i> -value	<i>r</i> -value	<i>p</i> -value	<i>r</i> -value	<i>p</i> -value
$\tau_{ThC}$ vs $F_x$	<b>0.19</b>	<b>0.06</b> <sup>(4/9)</sup>	<b>-0.90</b>	<b>&lt;0.001</b> <sup>(10/10)</sup>	<b>-0.14</b>	<b>0.17</b> <sup>(1/6)</sup>
$\tau_{ThC}$ vs $F_y$	0.04	0.71 <sup>(4/9)</sup>	-0.63	<0.001 <sup>(8/10)</sup>	0.39	<0.001 <sup>(2/6)</sup>
$\tau_{ThC}$ vs $F_z$	0.85	<0.001 <sup>(9/9)</sup>	0.52	<0.001 <sup>(7/10)</sup>	0.08	0.46 <sup>(1/6)</sup>
$\tau_{CTr}$ vs $F_x$	0.76	<0.001 <sup>(9/9)</sup>	-0.21	0.04 <sup>(4/10)</sup>	-0.83	<0.001 <sup>(6/6)</sup>
$\tau_{CTr}$ vs $F_y$	0.66	<0.001 <sup>(9/9)</sup>	0.25	0.01 <sup>(5/10)</sup>	0.04	0.70 <sup>(5/6)</sup>
$\tau_{CTr}$ vs $F_z$	<b>0.96</b>	<b>&lt;0.001</b> <sup>(9/9)</sup>	<b>1.00</b>	<b>&lt;0.001</b> <sup>(10/10)</sup>	<b>0.93</b>	<b>&lt;0.001</b> <sup>(6/6)</sup>
$\tau_{FTi}$ vs $F_x$	<b>0.28</b>	<b>&lt;0.01</b> <sup>(6/9)</sup>	<b>0.07</b>	<b>0.47</b> <sup>(2/10)</sup>	<b>0.91</b>	<b>&lt;0.001</b> <sup>(6/6)</sup>
$\tau_{FTi}$ vs $F_y$	0.37	<0.001 <sup>(4/9)</sup>	-0.37	<0.001 <sup>(7/10)</sup>	-0.85	<0.001 <sup>(6/6)</sup>
$\tau_{FTi}$ vs $F_z$	-0.34	<0.001 <sup>(5/9)</sup>	-0.87	<0.001 <sup>(7/10)</sup>	-0.82	<0.001 <sup>(6/6)</sup>

<sup>a</sup>The superscripts following the *p*-values denote the number of individuals with the same correlation result (positive, negative, or no correlation) as the grand means. Correlations set in bold are reported in table 1 of the main manuscript.

### (b) Medio-lateral balance

In addition to body weight support and propulsion, the control of medio-lateral balance is a third important motor task during walking. It is particularly important if a narrow base of support and a centre of mass high above the ground increase the risk of falling sideways, like in humans [10].

In the stick insect, all legs contributed to the control of medio-lateral balance with lateral forces during straight walking (figures 2–4 of the main manuscript). Peak forces were similarly high in all legs, but differed in direction ( $-0.7 \pm 0.2$  mN in the hind leg,  $-0.9 \pm 0.4$  mN in the middle leg, and  $0.6 \pm 0.1$  mN in the front leg; grand mean  $\pm$  s.d. of animal means). Hind legs mainly pushed outward ( $F_y < 0$ ; figure 2*b*), front legs mainly pulled inward ( $F_y > 0$ ; figure 4*b*), and middle legs first pulled inward, then pushed outward (figure 3*b*). These patterns confirm previous findings in the stick insect [4], but are quite different from those observed in sprawled-posture animals moving at faster forward velocities. Cockroaches and geckos, for example, push all legs outward during level running [11,12], possibly to achieve dynamic self-stabilisation [13]. Notably, however, both animals change the direction of the lateral force to inward pulling during climbing [14,15]. Pulling forces of the stick insect during walking may therefore be related to their climbing behaviour in nature, where these forces likely aid

attachment mechanisms [16,17].

Because stick insects moved their legs considerably backward during the stance phase, lateral forces were not attributable to the action of any one leg joint alone (table S2). Direct positive correlations between time courses of joint torques and lateral forces were weak even for torques at the FTi joints. In fact, correlations were strongest with torques at the CTr joint of the hind leg (table S2). At this joint, large torques toward depression resulted in backward and outward directed forces, while flexion torques at the FTi joint counteracted a further extension of the leg such that forces could be transmitted to the ground (see also figure 2c).

## SUPPLEMENTARY REFERENCES

- 1 Wells, R. P. 1981 The projection of the ground reaction force as a predictor of internal joint moments. *Bull. Prosthet. Res.* **18**, 15–19.
- 2 Biewener, A. A. & Full, R. J. 1992 Force platform and kinematic analysis. In *Biomechanics: structures and systems: a practical approach* (ed. A. A. Biewener), pp. 24–73. New York: Oxford University Press.
- 3 Featherstone, R. 2008 *Rigid body dynamics algorithms*. New York, NY: Springer.
- 4 Cruse, H. 1976 The function of the legs in the free walking stick insect *Carausius morosus*. *J. Comp. Physiol. A* **112**, 235–262. (doi:10.1007/BF00606541)
- 5 Cruse, H. & Bartling, C. 1995 Movement of joint angles in the legs of a walking insect, *Carausius morosus*. *J. Insect Physiol.* **41**, 761–771. (doi:10.1016/0022-1910(95)00032-P)
- 6 Theunissen, L. M., Bekemeier, H. H. & Dürr, V. 2015 Comparative whole-body kinematics of closely related insect species with different body morphology. *J. Exp. Biol.* **218**, 340–352. (doi:10.1242/jeb.114173)
- 7 Büschges, A. 2012 Lessons for circuit function from large insects: towards understanding the neural basis of motor flexibility. *Curr. Opin. Neurobiol.* **22**, 602–608. (doi:10.1016/j.conb.2012.02.003)
- 8 Dürr, V., Schmitz, J. & Cruse, H. 2004 Behaviour-based modelling of hexapod locomotion: linking biology and technical application. *Arthropod. Struct. Dev.* **33**, 237–250. (doi:10.1016/j.asd.2004.05.004)
- 9 Labonte, D. & Federle, W. 2013 Functionally different pads on the same foot allow control of attachment: Stick insects have load-sensitive heel pads for friction and shear-

- sensitive toe pads for adhesion. *PLOS one* **8**, e81943. (doi:10.1371/journal.pone.0081943)
- 10 Winter, D. A. 1995 Human balance and posture control during standing and walking. *Gait Posture* **3**, 193–214. (doi:10.1016/0966-6362(96)82849-9)
  - 11 Full, R. J., Blickhan, R. & Ting, L. H. 1991 Leg design in hexapedal runners. *J. Exp. Biol.* **158**, 369–390.
  - 12 Chen, J. J., Peattie, A. M., Autumn, K. & Full, R. J. 2006 Differential leg function in a sprawled-posture quadrupedal trotter. *J. Exp. Biol.* **209**, 249–259.
  - 13 Kubow, T. M. & Full, R. J. 1999 The role of the mechanical system in control: a hypothesis of self-stabilization in hexapedal runners. *Phil. Trans. R. Soc. B.* **354**, 849–861. (doi:10.1098/rstb.1999.0437)
  - 14 Goldman, D. I., Chen, T. S., Dudek, D. M. & Full, R. J. 2006 Dynamics of rapid vertical climbing in cockroaches reveals a template. *J. Exp. Biol.* **209**, 2990–3000.
  - 15 Autumn, K., Hsieh, S. T., Dudek, D. M., Chen, J., Chitaphan, C. & Full, R. J. 2006 Dynamics of geckos running vertically. *J. Exp. Biol.* **209**, 260–272.
  - 16 Zill, S. N., Chaudhry, S., Exter, A., Büschges, A. & Schmitz, J. 2014 Positive force feedback in development of substrate grip in the stick insect tarsus. *Arthropod. Struct. Dev.* **43**, 441–455. (doi:10.1016/j.asd.2014.06.002)
  - 17 Zill, S. N., Chaudhry, S., Büschges, A. & Schmitz, J. Force feedback reinforces muscle synergies in insect legs. *Arthropod. Struct. Dev.* In Press. (doi:10.1016/j.asd.2015.07.001)